

RESEARCH

Open Access



CHI3L1 mediates radiation resistance in colorectal cancer by inhibiting ferroptosis via the p53/SLC7A11 pathway

Ming Jin^{1†}, Hui Liu^{1†}, Zhen Zheng¹, Shuai Fang², Yang Xi³ and Kaitai Liu^{1*}

Abstract

Background Radiotherapy is a key treatment for colorectal cancer (CRC), particularly rectal cancer; however, many patients are resistant to radiation. While it has been shown that CHI3L1 is associated with CRC progression, its specific function and regulatory mechanisms in radiation resistance remain unclear.

Methods The levels of CHI3L1 in CRC and normal tissue samples were obtained from The Cancer Genome Atlas (TCGA) and Gene Expression Omnibus (GEO) datasets. To assess the effects of CHI3L1 on CRC cell proliferative, migratory, and invasive capacities, Cell Counting Kit-8 (CCK-8) and Transwell assays were performed. Radiation resistance in CRC cells with varying CHI3L1 expression levels was evaluated through colony formation assay. Western blot and immunofluorescence analyses were conducted to explore the correlation between CHI3L1 and p53 expression levels. Ferroptosis was assessed by determining reactive oxygen species (ROS), malondialdehyde (MDA), and glutathione (GSH) concentrations in cells with different CHI3L1 expression levels, and a xenograft mouse model was used to identify the molecular mechanisms of ferroptosis in vivo.

Results Significant CHI3L1 upregulated was observed in CRC tissues and was associated with promotion of malignant cell behaviors. The number of colonies in CHI3L1-overexpressing groups was significantly greater than that in the control groups following radiation, indicating increased radiation resistance in the former group. Furthermore, CHI3L1 overexpression was associated with p53 downregulation and elevated p53 ubiquitination. Notably, CHI3L1 inhibited the ferroptosis of CRC cells by suppressing p53 expression through the p53/SLC7A11 signaling pathway.

Conclusions CHI3L1 overexpression promotes the proliferation, migration, invasion, and radiation resistance of CRC cells. Elevated CHI3L1 expression is associated with increased p53 ubiquitination and SLC7A11 upregulation. CHI3L1 promotes radiation resistance by suppressing ferroptosis in CRC cells through the p53/SLC7A11 axis.

Keywords CHI3L1, Radiation resistance, P53, SLC7A11, Colorectal cancer, Ferroptosis

[†]Ming Jin and Hui Liu equal contribution.

*Correspondence:

Kaitai Liu

lkt1982@126.com

Full list of author information is available at the end of the article



Introduction

Colorectal cancer (CRC), encompassing both rectal and colon cancer, is a common gastrointestinal malignancy worldwide [1]. Radiotherapy is a critical component of multimodality therapy that extend the overall survival time of patients with CRC [2]. Neoadjuvant chemoradiotherapy (NCRT) is a key treatment for patients for whom anal function preservation during surgery is difficult and has been shown to significantly reduce the local recurrence rate of rectal cancer [3]. However, the low rate of pathological complete response (pCR) rate after NCRT suggests that a significant number of patients develop resistance to radiotherapy, leading to a poor prognosis [4–6].

Chitinase-3-like protein 1 (CHI3L1) or YKL-40, is reported to contribute to tumor growth across various cancer types. Elevated CHI3L1 levels are linked with radiation resistance in glioblastoma, which correlates with a poorer prognosis [7, 8]. However, the precise function and regulatory pathways of CHI3L1 in radiation resistance of CRC cells remain to be clarified. In recent years, studies have revealed a close link between radiation resistance and ferroptosis [9, 10]. However, limited research has reported the relationship between CHI3L1 and ferroptosis. P53, an important tumor suppressor gene, has been demonstrated to play a critical role in radiation resistance, especially in lung and prostate cancers, where it influences cellular responses to radiation by modulating DNA damage signaling, autophagy, and apoptosis pathways [11, 12]. Recent findings have shown the important role of p53 in ferroptosis [13]. Our previous research demonstrated that CHI3L1 overexpression promoted CRC cell proliferation by inhibiting p53 activity [14]. Therefore, we suggest that CHI3L1 may affect ferroptosis by regulating p53, leading to radiation resistance in CRC.

The aim of the present study was to assess the role of CHI3L1 overexpression in CRC cells, specifically its impact on cell proliferation, migration, invasion, and radiation resistance. This study also aimed to explore the potential mechanism by which CHI3L1 promotes radiation resistance, focusing on its regulation of ferroptosis through the p53/SLC7A11 axis.

Materials and methods

Clinical data

Data on CHI3L1 in CRC cases were collected from publicly available databases, specifically The Cancer Genome Atlas (TCGA) and Gene Expression Omnibus (GEO). For the TCGA cohort, gene expression profiles were studied in 620 CRC tissues compared with 789 adjacent normal tissues, while GSE31279 and GSE24550 were involved in our analysis from GEO database. In addition to this

database-derived data, the study also included 82 paired tissue samples, which were preserved in our laboratory for further analysis. The Ethics Committee of Ningbo Medical Center Lihuili Hospital granted ethical approval for this investigation.

Cell lines and cell culture

The human CRC cell lines SW480 and HCT116 were used in this study. Cells were grown in DMEM enriched with 10% fetal bovine serum at 37 °C with 5% CO₂. Subculturing was performed every 2–3 days at a 1:3 ratio.

Cell transfection

For CHI3L1 knockdown and overexpression, inhibitors and synthetic analogs were designed. According to the instructions, these inhibitors or analogs were mixed in serum-free medium to achieve a final concentration of 50 nM, followed by the addition of 5 μL of Lipofectamine 2000 to transfect SW480 and HCT116 cells. After 4 h, the cells were transferred to normal medium for continued culture.

Cell counting Kit-8 (CCK8) assay

Cells were harvested and prepared for suspension culture. They were inoculated in a 96-well plate at 5 × 10³ cells per well and grown at 37 °C with 5% CO₂ to allow cell adherence and proliferation. To monitor cell growth over time, cells were grown for 0, 24, 48, 72, and 96 h after which 10 μL of CCK8 reagent was introduced into each well to assess cell viability, as the reagent undergoes a colorimetric reaction proportional to the cell viability. After incubation for 2 h at 37 °C, absorbance at 450 nm were read. The results were used to determine the growth pattern as well as the viability of the cells over the specified time intervals.

Transwell migration and invasion assays

The migratory and invasive potential of CRC cells was assessed through Transwell assays. Cells that grew well after transfection were counted, and a suspension of 2 × 10⁵ cells/mL was prepared using serum-free culture medium, adding 200 μL to each upper chamber. For the migration assay, the cell suspension was carefully pipetted into the upper chamber, while for the invasion assay, the porous membrane was first coated with Matrigel and allowed to solidify before the cell suspension was added to the upper chamber. The lower chamber was then filled with medium supplemented with 20% serum as a chemoattractant. Incubation for 24 h allowed cells with migratory and invasive properties to move through the membrane towards the lower chamber. Residual cells on the upper membrane surface were then removed carefully while those that migrated were fixed, stained, and

visualized using a microscope. The migrated and invasive cells were counted in multiple fields of view to ensure accurate results. The cell counts were then analyzed to assess the migratory and invasive capabilities of the cells.

Colony formation assay

A colony formation assay was carried out to assess the colony-forming capability of CRC cells after exposure to various radiation doses. To prepare the substrate layer, 1.2% agarose was combined with 2×DMEM in a 1:1 volume ratio to prepare a 0.6% agarose solution, which was then dispensed at 1.4 mL per well into six-well plates and allowed to solidify. The cell count was adjusted to 10,000 cells/mL. For the upper layer, 0.6% agarose was again mixed with 2×DMEM at a 1:1 ratio to produce a 0.3% agarose solution. Then, 1 mL of this upper agarose was mixed with 500 μL of the cell suspension, resulting in 5,000 cells per well, and added to each well before solidification. The cells were then grown under normal conditions for 2–3 weeks. Finally, colony images were captured and analyzed.

Cell immunofluorescence

Six-well plates were seeded with 5000 cells per well, allowing the cells to attach. Following aspiration of the media, the cells were fixed with 1 mL of 4% paraformaldehyde and incubated at room temperature for 20 min to preserve cellular structures. Following fixation, the cells were treated with primary antibodies targeting CHI3L1 and p53 to detect their expression. After antibody incubation, the cells were stained with DAPI to label the nuclei. Fluorescence microscopy was then employed to capture images.

The detection of reactive oxygen species (ROS), malondialdehyde (MDA), and glutathione (GSH)

Flow cytometry was used to quantify intracellular ROS. Cells in a diluted DCFH-DA solution were incubated at 37 °C for 20 min after which they were rinsed three times with serum-free medium for removal any uninternalized DCFH-DA. Flow cytometric analysis was then performed to measure ROS levels. Additionally, assay kits for ROS, MDA, and GSH were also used following the provided directions.

Real-time PCR

Cells were processed to isolate total RNA with the TRIzol method, followed by reverse transcription into cDNA. For quantitative PCR, the reaction mix was prepared in accordance with the SYBR Green protocol. Each 20 μL reaction included 10 μL of SYBR Green Master Mix, 0.4 μL of the forward and reverse primers, 2 μL of cDNA, and deionized water. The PCR conditions were an initial

denaturation step at 95 °C for 30 s (s), 40 amplification cycles comprising denaturation at 95 °C for 10 s, annealing at 58 °C for 30 s, and extension at 72 °C for 30 s. Samples were run in triplicate to ensure accuracy and reproducibility. Relative gene expressions were assessed using the $2^{-\Delta\Delta C_t}$ method, allowing for the comparison of expression levels between experimental and control groups.

Western blot

The HCT116 and SW480 cell lysates were prepared in SDS lysis buffer to extract total protein. For the quantification of proteins, a BCA protein assay kit was employed. Proteins were added to loading buffer and separated on SDS-PAGE, followed by transfer to a PVDF membrane, which was blocked and treated with primary antibodies overnight at a temperature of 4 °C. The blots were then rinsed three times with TBST and treated with a secondary antibody for a period of 1 h. After washing, enhanced chemiluminescence substrates were applied to visualize the target protein expression.

Coimmunoprecipitation

Firstly, cells were lysed using a cell lysis buffer to obtain a sample containing the target protein. Then, magnetic beads conjugated with specific antibodies were added to the sample, allowing the target protein to be precipitated. After eluting the protein with elution buffer, the protein complexes were separated using SDS-PAGE. Subsequently, Western Blot analysis was performed to detect the presence of the target protein.

Cell line-derived xenograft model

BALB/c nude mice (four-week-old) were used to develop tumor models. CRC cells, treated with si-CHI3L1 or si-NC (1×10^7 cells/mL, 100 μL), were injected subcutaneously into the abdominal region of the mice. After two weeks of tumor formation, the mice underwent radiation treatment and were monitored until the tumors reached a measurable size. Tumor tissues were then harvested for further analysis.

Immunohistochemistry (IHC)

The levels and cellular localization of target proteins in CRC tissues were assessed using IHC analysis. The IHC score was employed to semi-quantitatively assess the expression levels of target proteins in CRC and control tissue samples. Antibodies against CHI3L1, p53, and SLC7A11 were used in the analysis.

Statistical analysis

Differences between groups were assessed using *t*-tests. Error bars in the figures indicated the Standard Error of

the Mean (SEM). All data were presented as mean ± SEM. Statistical significance was defined as a *p*-value below 0.05. Data analysis was conducted with SPSS (version 22.0) and GraphPad Prism (version 8.0) to ensure precise data interpretation and visualization.

Results

High expression of CHI3L1 in CRC tissues

This study initially assessed CHI3L1 expression levels in CRC tissues using data from the TCGA and GEO databases and revealed a markedly higher CHI3L1 levels in CRC tissues relative to adjacent normal tissues (Fig. 1A, B). On the basis of previous research, the sample size was expanded to confirm elevated CHI3L1 levels in 82 matched CRC tissue samples (Fig. 1C). Western blot analysis of five paired samples further validated CHI3L1 overexpression in CRC tissues (Fig. 1D). In addition, elevated CHI3L1 was observed in CRC cell lines, including SW480 and HCT116 [14].

CHI3L1 overexpression increased cell proliferation, migration, and invasion of CRC cells

To investigate the effects of CHI3L1 on CRC tumorigenic behavior, CCK-8 and Transwell assays were performed.

CHI3L1 levels in the cells were modulated through CHI3L1 knockdown or overexpression (Fig. 2A, B). The CCK-8 assay displayed that CRC cell proliferation was significantly reduced with CHI3L1 knockdown and increased with CHI3L1 overexpression (Fig. 2C). Similarly, Transwell assays showed a significant suppression of the invasion and migration of HCT116 and SW480 cells in the CHI3L1-knockdown groups, whereas these processes were significantly promoted in the CHI3L1-overexpression groups (Fig. 2D, E). Meanwhile, we also detected through CCK-8 and Transwell assays that in the CHI3L1 knockdown groups, the proliferation, migration, and invasion capabilities of HCT116 and SW480 cells were restored upon simultaneous overexpression of CHI3L1 (Figure S1A-F). Overall, these findings suggested that CHI3L1 was crucial for promoting CRC cell proliferation, migration, and invasion.

CHI3L1 overexpression promoted the radiation resistance of CRC cells

To assess the correlation between CHI3L1 expression and radiation resistance, radiation-resistant CRC cell lines (HCT116R and SW480R) were first established as previously described [15]. These radiation-resistant

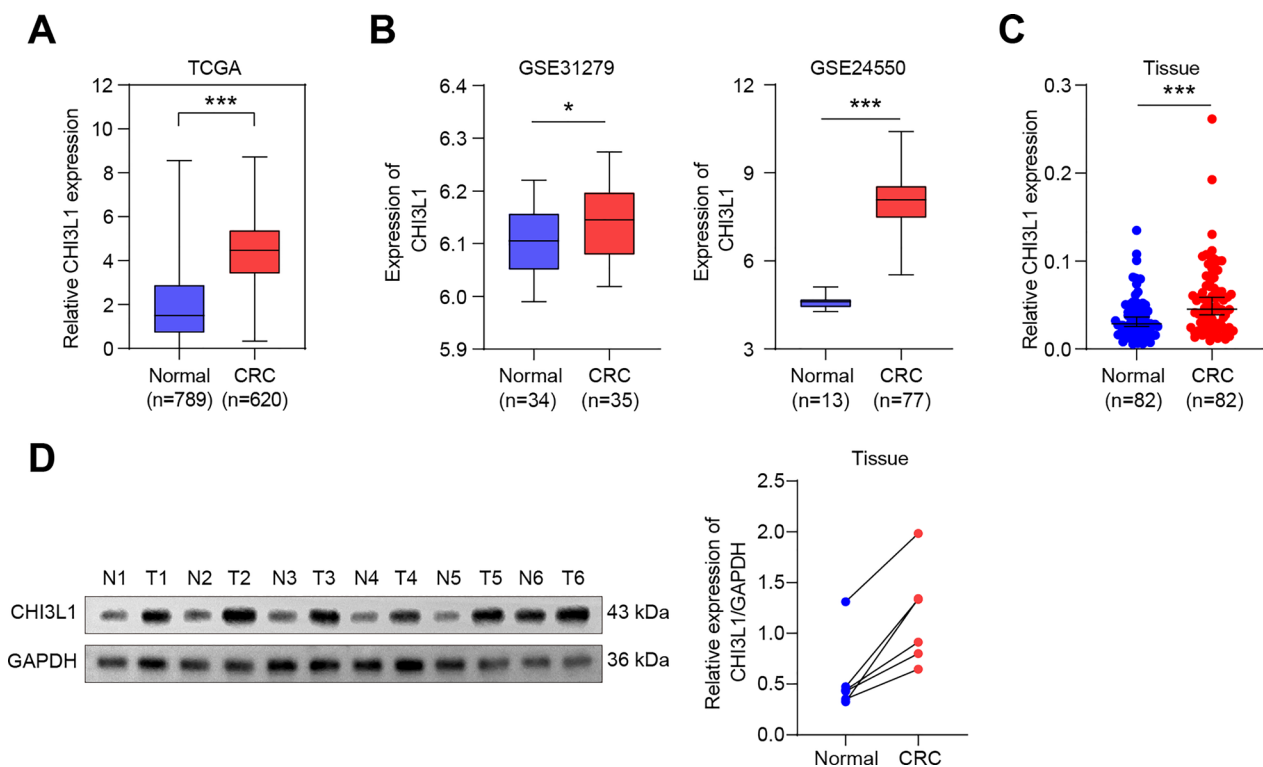


Fig. 1 The expression levels of CHI3L1 in CRC tissues. **A, B** CHI3L1 expression data from TCGA and GEO database. **C** qRT-PCR analysis of CHI3L1 levels in CRC tissues and paired normal tissues (*n* = 82). **D** Western blot analysis of CHI3L1 protein levels in CRC tissues and paired normal tissues (*n* = 6). **P* < 0.05, ***P* < 0.01, ****P* < 0.001

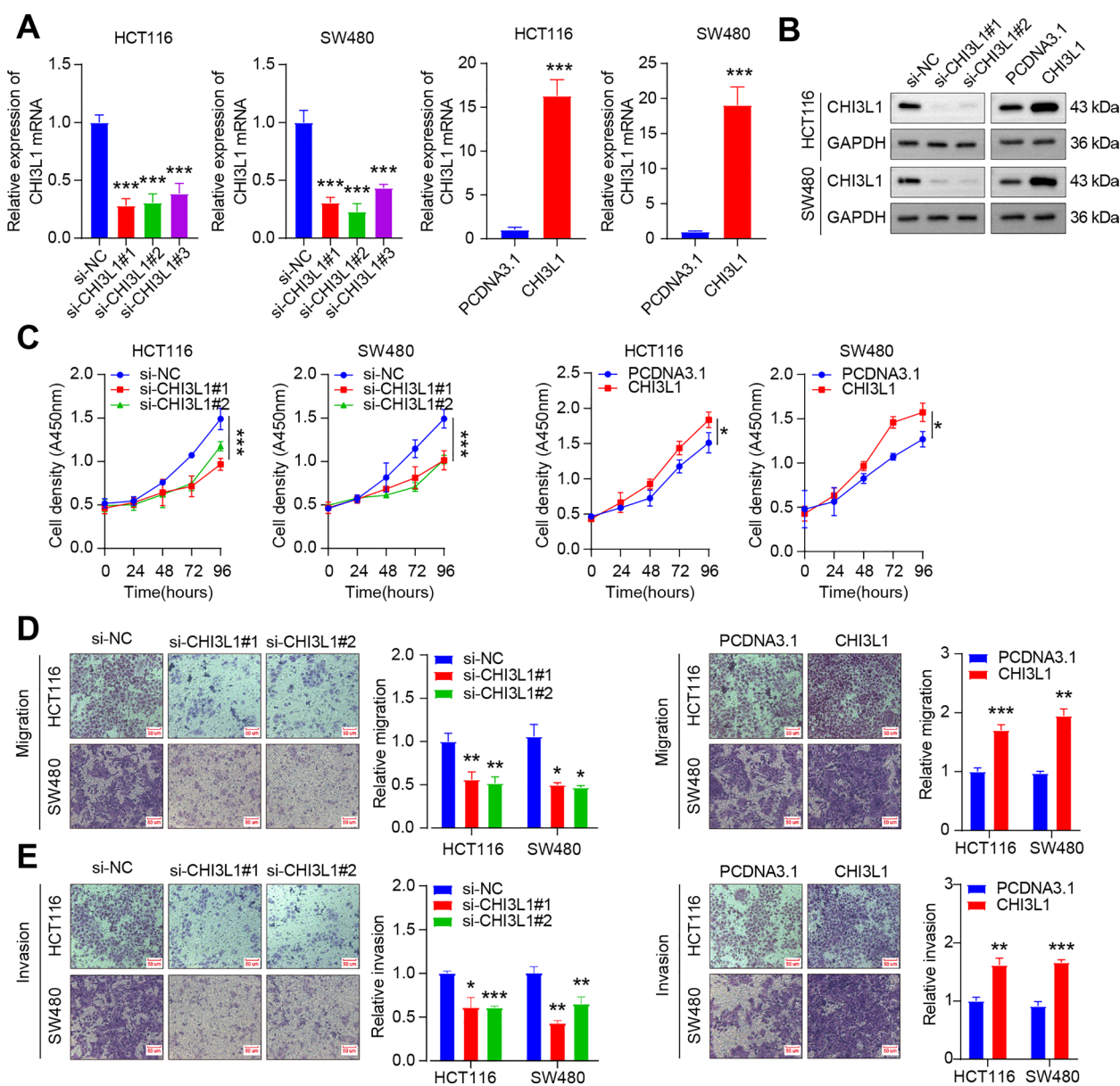


Fig. 2 Elevated CHI3L1 expression enhanced proliferation, migration, and invasive capabilities in CRC cells. **A, B** The efficiency of CHI3L1 overexpression and knockdown that verified by qRT-PCR and Western blot. **C** CCK8 and **D, E** Transwell assays were performed to assess the impact of CHI3L1 on the migration and invasion of CRC cells. * $P < 0.05$, ** $P < 0.01$, *** $P < 0.001$

lines presented elevated CHI3L1 expression levels (Fig. 3A). A colony formation assay was performed to examine the link between CHI3L1 expression and radiation resistance in CRC cells. The results showed that, across various doses of radiation (2, 4, 6, and 8 Gy), the number of colonies formed by the CHI3L1-knockdown cells was markedly lower than that formed by the control cells. However, the colony counts of the CHI3L1-overexpressing groups were significantly greater than those of the control groups (Fig. 3B). These findings

showed that CHI3L1 might enhance radiation resistance in CRC cells.

CHI3L1 overexpression was associated with increased levels of p53 ubiquitination

Our previous studies revealed that CHI3L1 overexpression significantly suppresses p53 levels [14]. Building on these findings, the present study further explored the relationship between CHI3L1 and changes in the p53 protein. Coimmunoprecipitation

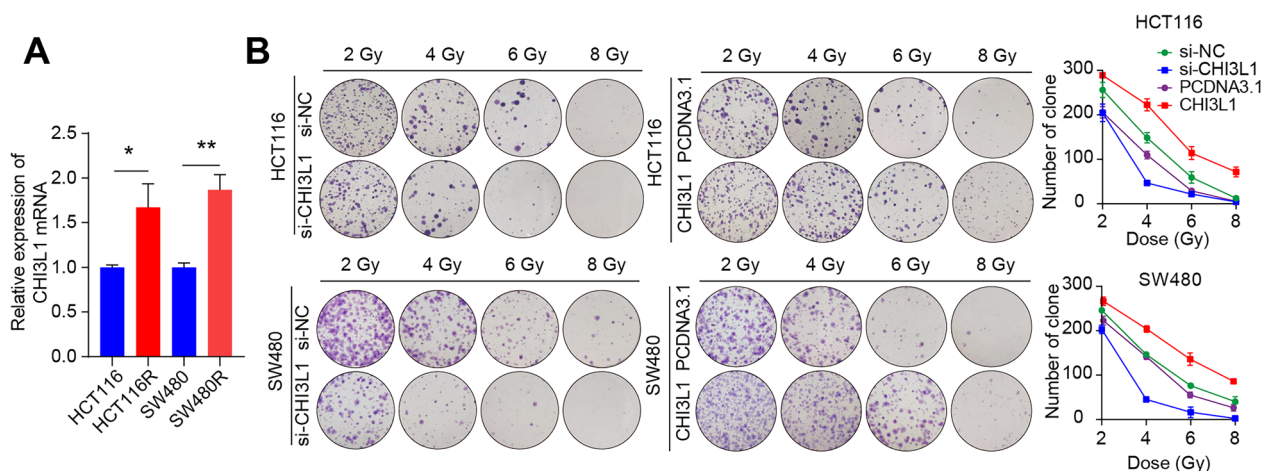


Fig. 3 CHI3L1 overexpression promoted the radiation resistance of CRC cells. **A** CHI3L1 expression levels in radiation-resistant CRC cell lines. **B** Colony formation assay conducted to count the number of colonies and elucidate the correlation between CHI3L1 expression and radiation resistance in CRC cells, across various doses of radiation (2, 4, 6, and 8 Gy). * $P < 0.05$, ** $P < 0.01$

data indicated a direct interaction between CHI3L1 and p53 (Fig. 4A), whereas immunofluorescence studies confirmed the colocalization of both proteins in CRC cells (Fig. 4B). The expression levels of CHI3L1 were inversely correlated with those of the p53 protein (Fig. 4C). However, at the mRNA level, changes in CHI3L1 did not significantly affect p53 mRNA levels (Fig. 4D). These findings suggested that, rather than affecting mRNA levels, CHI3L1 might reduce p53 expression through protein modifications.

Further investigations were conducted to explore the interaction between CHI3L1 and p53 ubiquitination. Cells were treated with the proteasome inhibitor MG132 (10 μ M) for 6 h to increase p53 ubiquitination, while the protein synthesis inhibitor cycloheximide (CHX) (180 μ M) was used to treat the cells for 6 h to reduce p53 ubiquitination. Compared with the control conditions, exposure to MG132 increased the p53 levels in CRC cells, with a less pronounced increase in the CHI3L1-overexpressing groups. In contrast, CHX treatment decreased p53 levels, with a much greater reduction in p53 levels in the CHI3L1-overexpressing groups than in the control groups (Fig. 4E, F). Similar experiments in CHI3L1-knockdown cells revealed that MG132 did not significantly increase p53 levels in these cells, while after CHX treatment, p53 levels in CHI3L1-knockdown cells were comparatively higher than those in control cells (Fig. 4G, H). Ubiquitination assays ultimately demonstrated that CHI3L1 overexpression was associated with increased p53 ubiquitination, whereas CHI3L1 knockdown correlated with reduced p53 ubiquitination (Fig. 4I).

CHI3L1 suppressed ferroptosis through the p53/SLC7A11 axis in CRC cells

Studies have shown that p53 may facilitate cell ferroptosis by suppressing the expression of SLC7A11 [13]. In our study, the levels of p53 were reduced in CRC tissues, especially when the sample size was expanded. However, SLC7A11 was overexpressed in these tissues (Fig. 5A, B). A marked negative association was found between p53 expression and both CHI3L1 and SLC7A11 expression. Furthermore, a strong positive correlation was found between CHI3L1 and SLC7A11 expression (Fig. 5C–E). Moreover, the SLC7A11 expression level increased following CHI3L1 overexpression but decreased after CHI3L1 knockdown (Fig. 6A).

Fer-1 was used to assess whether the ferroptosis induced by CHI3L1 knockdown could be mitigated. All experimental cells were treated with 10 μ M of Fer-1 for 24 h. The results of the CCK-8 assay showed that Fer-1 effectively reversed the suppression of cell growth caused by CHI3L1 knockdown (Fig. 6B). The levels of ROS, MDA, and GSH were measured as indicators of ferroptosis. Fer-1 counteracted the rise in ROS and MDA levels and the reduction in GSH levels resulting from CHI3L1 knockdown (Fig. 6C–F). Furthermore, erastin was used to promote ferroptosis, specifically, all experimental cells were treated with 10 μ M of erastin for 24 h prior to the experiments. The results indicated that erastin counteracted the effects of CHI3L1 overexpression, including the promotion of cell proliferation, the decrease in MDA and ROS levels, and the rise in GSH levels (Fig. 6G–K). Together, these

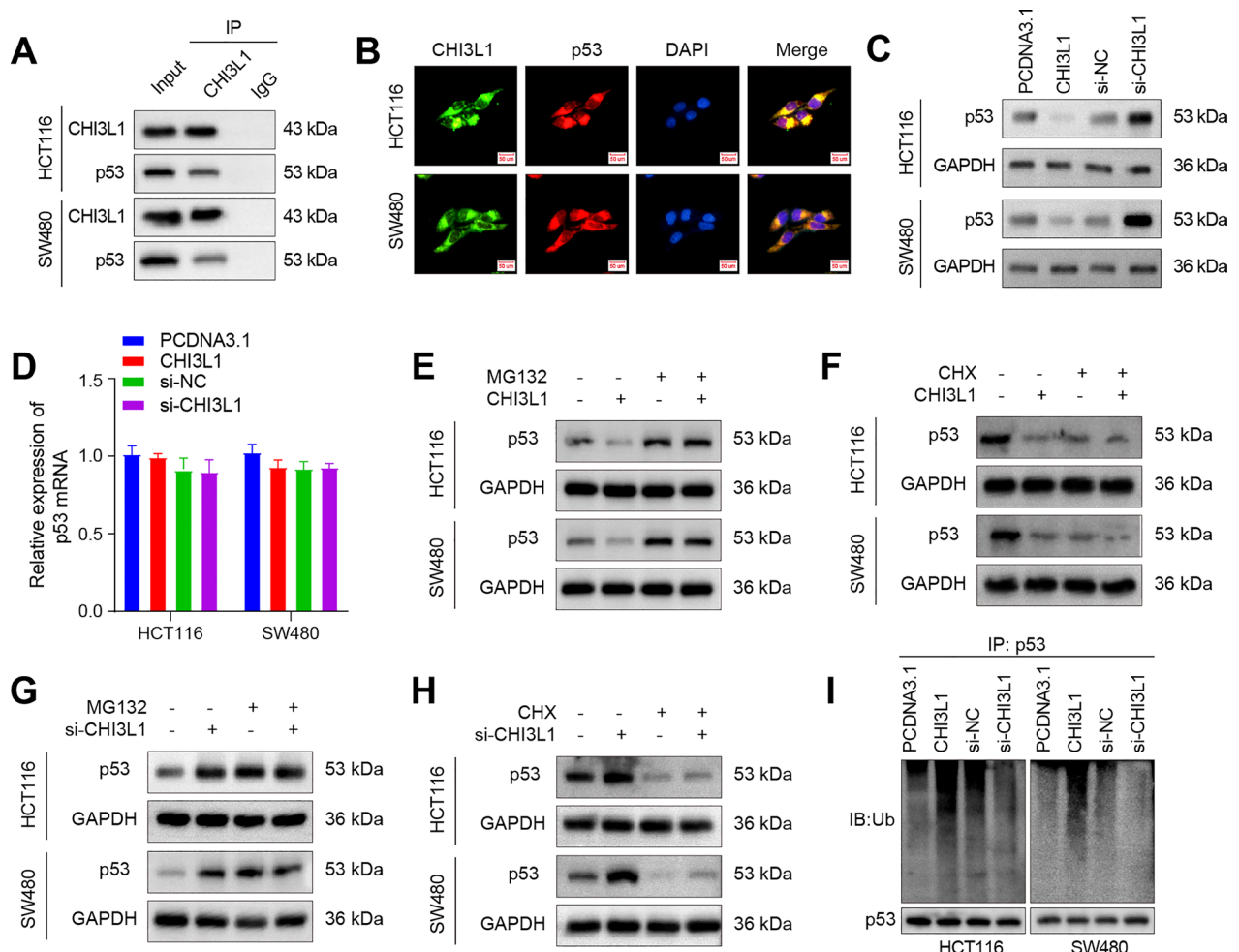


Fig. 4 CHI3L1 overexpression was associated with increased levels of p53 ubiquitination. **A, B** Coimmunoprecipitation results and **C** Western blot analysis revealed a direct interaction between CHI3L1 and p53. **D** Examination of p53 mRNA expression with varying CHI3L1 levels. **E–H** Western blot analysis of p53 protein levels following treatment with MG132 (10 μ M) and CHX (180 μ M). **I**) Ubiquitination assay for confirming the connection between CHI3L1 and p53

results indicated that CHI3L1 overexpression might suppress the ferroptosis of CRC cells.

The influence of CHI3L1/p53 on ferroptosis in CRC cells was further investigated. p53 knockdown resulted in increased cell proliferation, lowered ROS and MDA levels, and raised GSH levels. When CHI3L1 was additionally knocked down, cell proliferation was inhibited (Fig. 7A), and the changes in ROS, MDA, and GSH levels induced by p53 knockdown were reversed (Fig. 7B, C). These findings suggested that CHI3L1 mitigates ferroptosis in CRC cells by suppressing p53 expression. Furthermore, our study also found that SLC7A11 knockdown led to reduced cell proliferation, increased levels of ROS and MDA, and decreased levels of GSH. When CHI3L1 was overexpressed simultaneously, the cell proliferation capacity was restored (Figure S2A), and the SLC7A11 knockdown-induced changes in ROS,

MDA, and GSH levels were reversed (Figure S2B–C). These findings suggest that CHI3L1 alleviates ferroptosis in CRC cells by promoting SLC7A11 expression.

In vivo experiments were also performed to examine the effect of the CHI3L1/p53/SLC7A11 signaling pathway on ferroptosis in CRC cells. The results revealed that radiation effectively suppressed tumor growth in the mice, as both tumor volume and weight significantly decreased in the CHI3L1-knockdown groups compared with those in the control groups (Fig. 8A–C). The IHC analysis revealed that, following radiation, p53 expression increased and SLC7A11 expression decreased in the CHI3L1-knockdown groups (Fig. 8D). Collectively, the data suggested a potential role for CHI3L1 in preventing ferroptosis in CRC cells through the regulation of the p53/SLC7A11 axis.

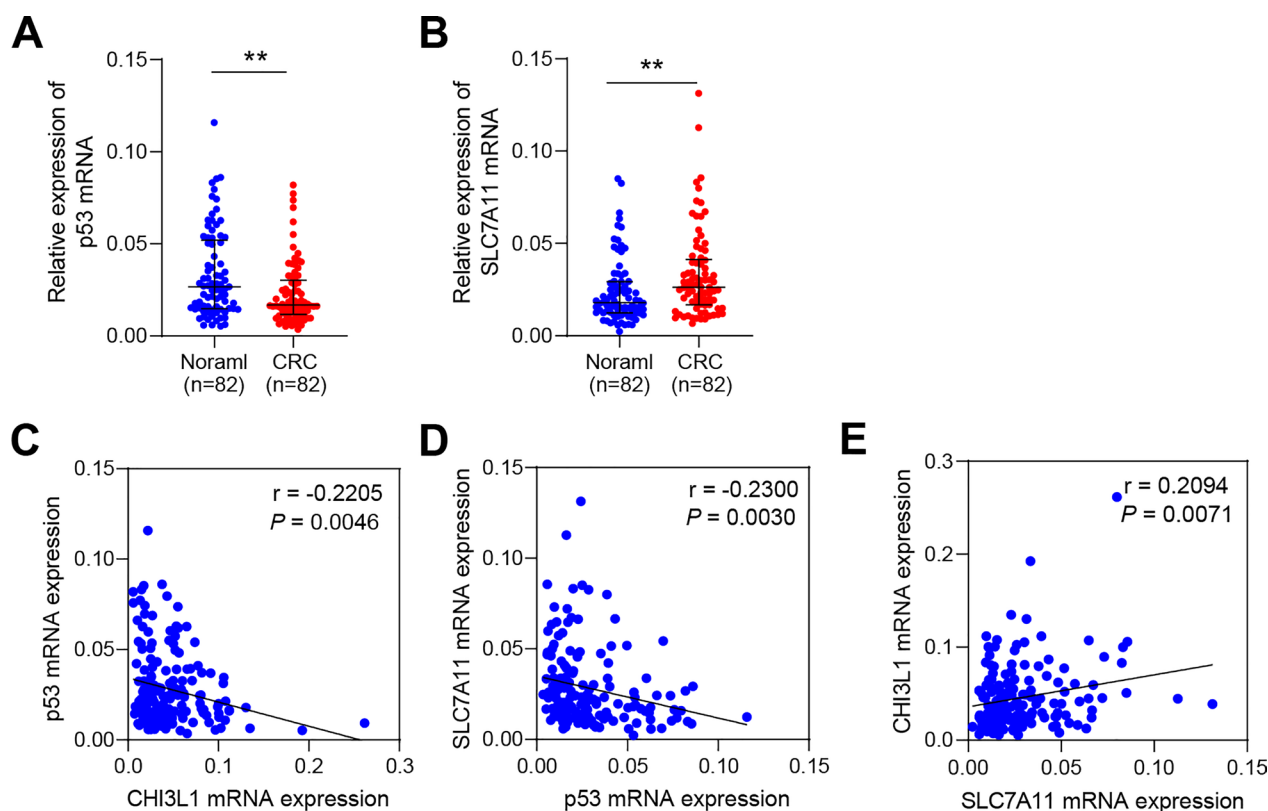


Fig. 5 Correlation among CHI3L1, p53 and SLC7A11. **A, B** The expression data of p53 and SLC7A11. **C–E** The correlation among CHI3L1, p53 and SLC7A11 expression levels. ** $P < 0.01$

Discussion

Both preoperative and postoperative radiation therapy significantly lower the risk of local recurrence and prolong the survival time of rectal cancer patients [16, 17]. However, despite the importance of radiotherapy for locally advanced rectal cancer, there is still less than one-fifth of the patients achieve pCR, which indicating that radiation resistance has emerged as one of the primary factors limiting the effectiveness of this treatment [4, 5]. CHI3L1 has been identified as a factor that promotes tumor growth in various types of cancer. The present study confirmed that CHI3L1 was overexpressed in CRC tissues with an expanded sample size. Furthermore, the study revealed that CHI3L1 overexpression promotes the proliferation, migration, and invasion of CRC cells.

Radiation-induced DNA damage can lead to molecular fractures, resulting in irreversible cell damage and even cell death, and poor outcomes of radiotherapy may result from the strong ability of cells to repair radiation damage [18]. In this study, the correlation between CHI3L1 and radiation resistance in CRC cells, along with the underlying molecular mechanism, was further explored. The results showed that the colony count in the CHI3L1-overexpressing CRC

cell lines was significantly greater than that in the control groups across various radiation doses, whereas the colony count was significantly lower in the CHI3L1-knockdown groups. Moreover, a significant association between CHI3L1 and alterations in p53 protein levels was observed. Recent research has underscored the potential role of p53 in radiation resistance. The efficacy of radiotherapy can be hindered by the high DNA damage repair capacity of certain cells [19]. The p53 protein plays an essential role in the signaling pathways that respond to DNA damage and in arresting the cell cycle following radiation exposure [11, 12, 20]. Interestingly, p53 also affects chromatin compaction, a key factor in DNA damage induction, making it an important indicator of radiation sensitivity [21, 22]. Previous reports have shown that the overexpression of CHI3L1 significantly suppresses p53 levels [14]. In the present study, a direct interaction between CHI3L1 and p53 was confirmed, with both proteins colocalizing in CRC cells. However, no significant differences in p53 mRNA levels were observed when CHI3L1 expression was altered. These findings suggested that, rather than altering mRNA levels, CHI3L1 might reduce p53 expression through protein modifications.

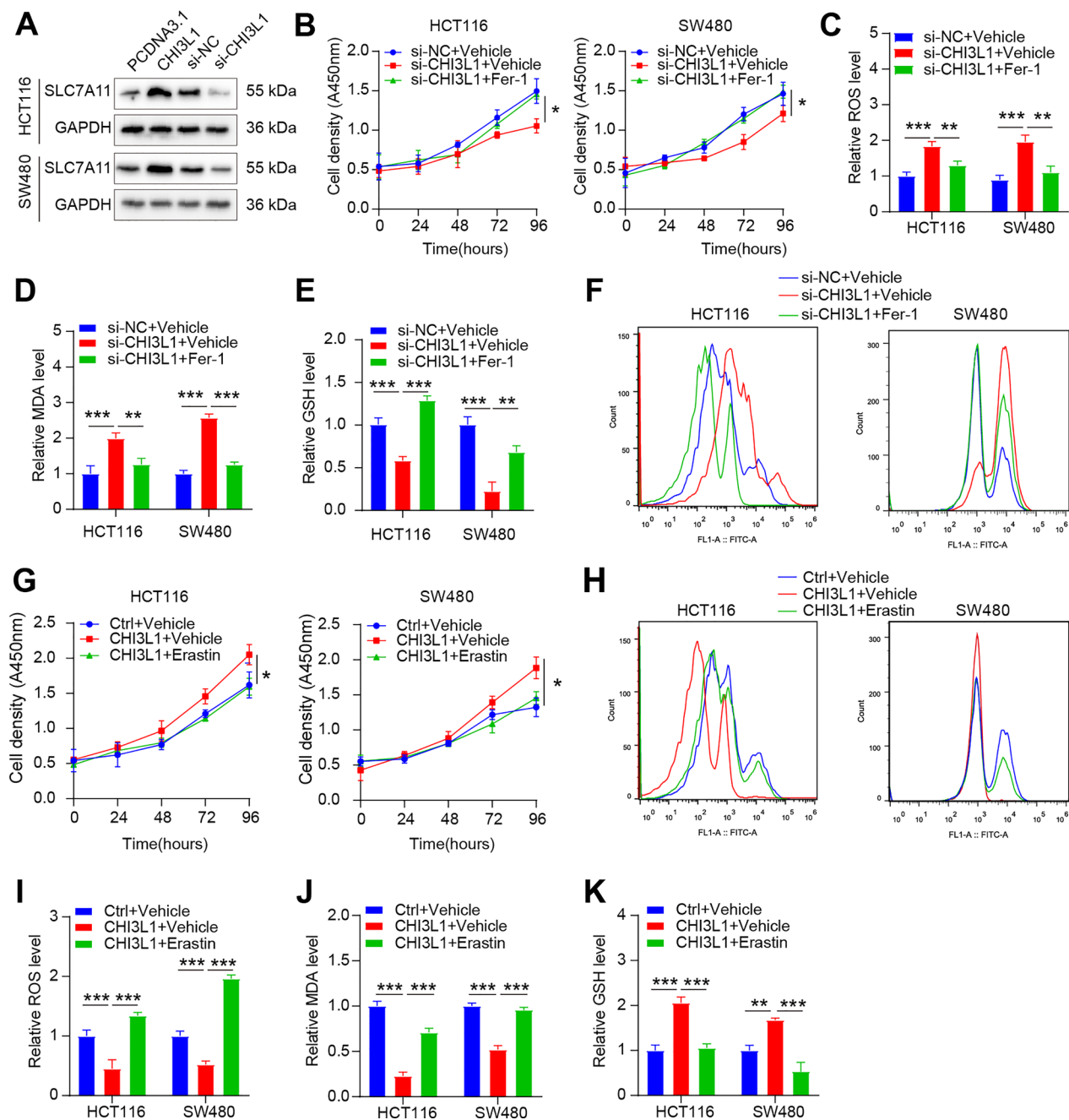


Fig. 6 CHI3L1 promoted the radiation resistance by reducing ferroptosis. **A** Analysis of SLC7A11 expression levels in response to CHI3L1 overexpression and knockdown. **B–F** Utilization of Fer-1 (10 μ M) to inhibit ferroptosis and evaluate the ability of CHI3L1 knockdown to induce ferroptosis and its potential reversal through the detection of ROS, MDA, and GSH concentrations in cells with different CHI3L1 expression levels. **G–K** Application of erastin (10 μ M) to augment ferroptosis. * $P < 0.05$, ** $P < 0.01$, *** $P < 0.001$

Post-translational modifications such as ubiquitination, phosphorylation, and acetylation are critical for regulating the structure and function of p53, significantly affecting its stability and activity [23]. Ubiquitination, particularly at the lysine residues of p53, is mediated by the ubiquitin ligase MDM2, inducing p53 degradation,

thereby maintaining low levels of p53 [24]. In lung cancer cells, WDR5 overexpression has been shown to positively regulate p53 expression by inhibiting its ubiquitination and stabilizing the protein [25]. Similarly, DAB2IP promotes p53 stability by preventing its degradation via the ubiquitin–proteasome pathway [26]. In the present study,

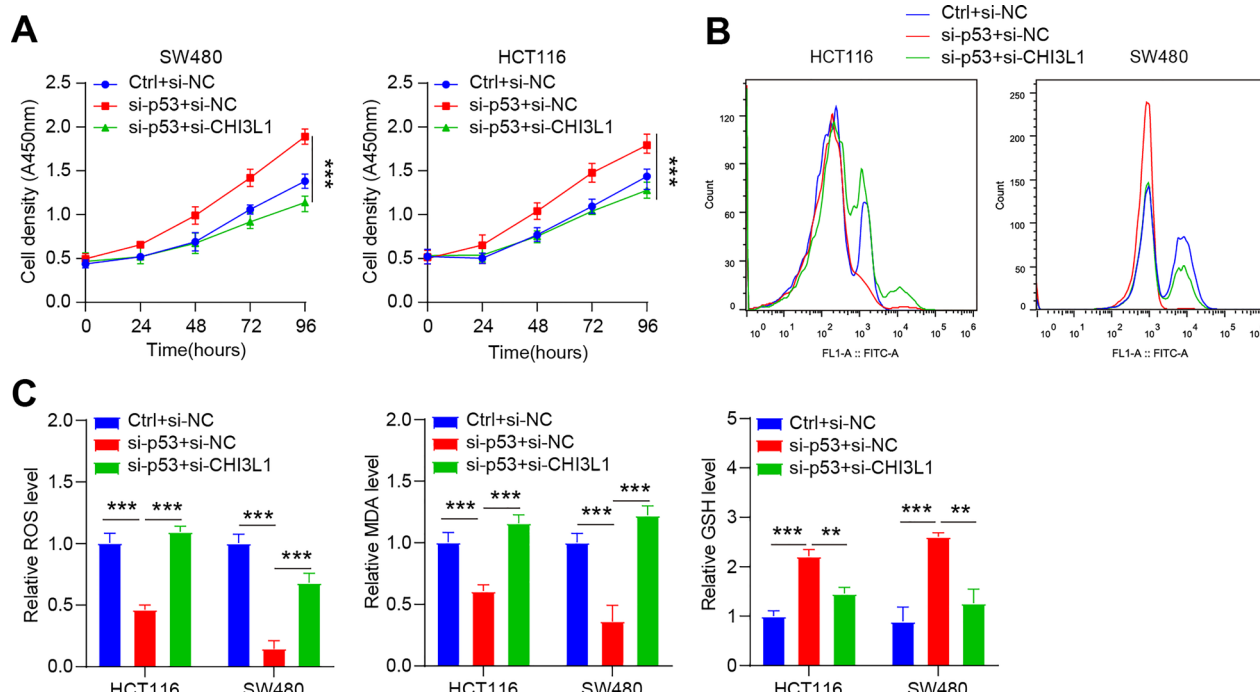


Fig. 7 The influence of CHI3L1/p53 on ferroptosis in CRC cells. **A** Analysis of cell proliferation under varying CHI3L1 and p53 expression levels. **B–C** Assessment of ROS, MDA, and GSH levels in relation to CHI3L1 expression changes. $**P < 0.01$, $***P < 0.001$

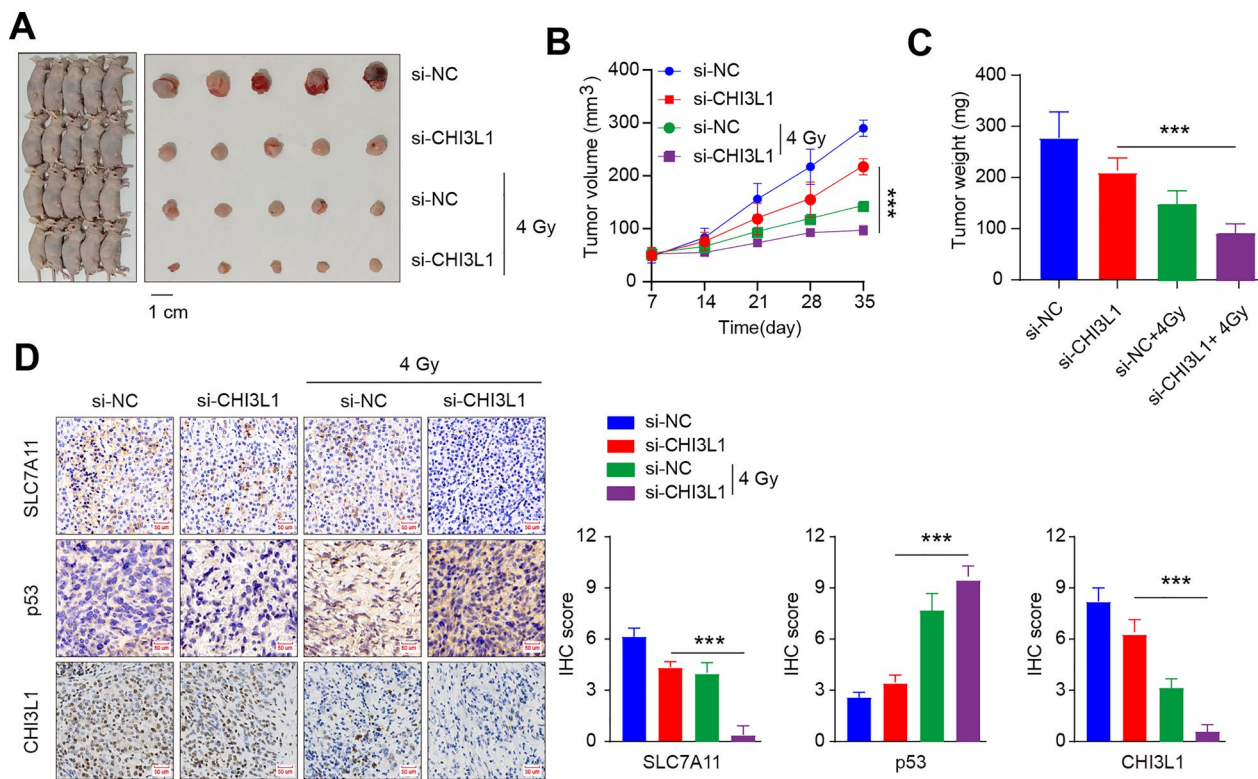


Fig. 8 In vivo exploration of the CHI3L1/p53/SLC7A11 pathway. **A–C** Development of a mice model for the study. **D** Following radiation, comparison of p53 and SLC7A11 expression levels in the CHI3L1-knockdown groups by IHC. $***P < 0.001$

the proteasome inhibitor MG132 was used to increase ubiquitination, and the protein synthesis inhibitor CHX was utilized to reduce the ubiquitination of p53. The results indicated that CHI3L1 overexpression was associated with increased p53 ubiquitination, whereas CHI3L1 knockdown led to decreased p53 ubiquitination. These findings suggested that CHI3L1 overexpression might increase p53 ubiquitination, thereby reducing p53 levels and potentially contributing to radiation resistance in CRC cells. This hypothesis is worthy of further investigation to better understand how CHI3L1 influences p53 stability and function, and reveal its impact on the radiation sensitivity of CRC cells.

Ferroptosis is a form of programmed cell death that involves iron-dependent lipid peroxidation, and its dysregulation is associated with tumor development [27, 28]. Studies have revealed that ionizing radiation can trigger ferroptosis in tumor cells, and simultaneously, it can also upregulate the expression of inhibitors that counteract ferroptosis. The modulation of ferroptosis is suggested to be crucial in determining the sensitivity of cancer cells to radiotherapy [9]. However, limited research has reported the relationship between CHI3L1 and ferroptosis. The p53 protein serves as an important bidirectional regulator of ferroptosis by modulating ROS, MDA, and GSH [29–31]. The degradation of p53 is essential for preventing ferroptosis and fostering tumor progression [32]. Thus, we aimed to explore the interplay between CHI3L1/p53 and ferroptosis in radiation resistance in CRC cells. In this study, a significant inverse association between the expression levels of p53 and CHI3L1, as well as between p53 and SLC7A11 was observed. These findings suggested that CHI3L1 overexpression could inhibit the ferroptosis of CRC cells. The ferroptosis inhibitor Fer-1 successfully attenuated cell growth inhibition, increased in ROS and MDA levels and prevented the reduction in GSH levels caused by CHI3L1 knockdown. Erastin, a ferroptosis inducer, was able to offset the effects induced by CHI3L1 overexpression. Moreover, p53 knockdown led to suppression of ferroptosis, which was attenuated when CHI3L1 was also knocked down. These results implied that CHI3L1 decreased cell ferroptosis in CRC cells by downregulating p53.

Recent studies have shown that radiation can cause SLC7A11 overexpression, which increases resistance to radiation by inhibiting ferroptosis through the p53/SLC7A11 signaling pathway [9, 13, 31, 33]. Preventing p53 degradation, specifically its ubiquitination, was found to lower SLC7A11 expression, thereby increasing oxidative stress and inducing ferroptosis [34, 35]. This study revealed a marked positive association between SLC7A11 and CHI3L1 expression levels. An increase in SLC7A11 expression was observed with CHI3L1

upregulation, whereas a decrease was observed when CHI3L1 was knocked down. In the CHI3L1-knockdown mice models after radiation, p53 expression was increased, and SLC7A11 expression was reduced. These results indicated that CHI3L1 might inhibit ferroptosis in CRC cells through regulation of the p53/SLC7A11 axis.

Although this study provides multiple insights, several limitations should be acknowledged. First, the sample size of patients included in the study was relatively small. Therefore, validation and further investigation in a larger cohort are warranted to better understand the relationship between CHI3L1 expression and the prognostic prediction of CRC. Additionally, more functional validations studies in animal models *in vivo* are necessary. The mechanisms and downstream regulatory effects of p53 ubiquitination on radiation sensitivity have not been extensively examined. Moreover, further research is needed to clarify the role of the CHI3L1/p53/SLC7A11 pathway in cell ferroptosis.

Conclusions

In conclusion, CHI3L1 is significantly overexpressed in CRC tissues. CHI3L1 overexpression promotes the proliferation, migration, invasion, and radiation resistance of CRC cells. Furthermore, elevated CHI3L1 expression is associated with increased p53 ubiquitination and SLC7A11 upregulation, suggesting that CHI3L1 may promote radiation resistance by suppressing ferroptosis through the p53/SLC7A11 signaling pathway.

Abbreviations

CRC	Colorectal cancer
CHI3L1	Chitinase-3-like protein 1
SLC7A11	Solute carrier family 7 member 11
TCGA	The Cancer Genome Atlas
GEO	Gene Expression Omnibus
ROS	Reactive oxygen species
MDA	Malondialdehyde
GSH	Glutathione
NCRT	Neoadjuvant chemoradiotherapy
pCR	Pathological complete response
PCR	Polymerase Chain Reaction
IHC	Immunohistochemistry
CHX	Cycloheximide
Fer-1	Ferostat-1
MDM2	MDM2 proto-oncogene
WDR5	WD repeat domain 5
DAB2IP	DAB2 interacting protein

Supplementary Information

The online version contains supplementary material available at <https://doi.org/10.1186/s12967-025-06378-6>.

Supplementary Material 1: Figure S1 Elevated CHI3L1 expression promoted proliferation, migration and invasive capabilities in CRC cells. CCK-8 detection showed that CHI3L1 knockdown could inhibit the proliferation of CRC cells, while overexpression of CHI3L1 restored cell proliferation ability. Transwell assay detected that overexpression of CHI3L1 restored the migration and invasion ability of CRC cells. * $P < 0.05$, ** $P < 0.01$.

Supplementary Material 2: Figure S2 The influence of CHI3L1/SLC7A11 on ferroptosis in CRC cells. Evaluation of cell proliferation in response to altered expression levels of CHI3L1 and SLC7A11. Measurement of ROS, MDA, and GSH levels in association with changes in CHI3L1 expression. * $P < 0.05$, ** $P < 0.01$, *** $P < 0.001$.

Acknowledgements

Not applicable.

Author contributions

LKT conceived and designed the experiments. FS, LKT and JM performed the experiments. FS, JM, LH and ZZ analyzed and interpreted the data. LKT and XY acquired funding and supervised the project. JM, LH, FS and LKT drafted and revised the paper. All authors reviewed and approved the final manuscript.

Funding

This study was supported by the Keynote Research Project of Ningbo City [2023Z171]; the Natural Science Foundation of Zhejiang Province [LY21H160013].

Availability of data and materials

Data are available from the corresponding author as required.

Declarations

Ethics approval and consent to participate

This study was approved by the Ethical Committee of Ningbo Medical Center Lihuilu Hospital.

Consent for publication

All listed authors consent to the submission.

Competing interests

The authors declare no competing interests.

Author details

¹Department of Radiation Oncology, The Affiliated Lihuilu Hospital of Ningbo University, Ningbo, Zhejiang, China. ²The Affiliated Hospital of Medical School of Ningbo University, Ningbo, Zhejiang, China. ³Department of Biochemistry and Molecular Biology, School of Basic Medical Sciences, Health Science Center, Ningbo University, Ningbo, Zhejiang, China.

Received: 15 January 2025 Accepted: 12 March 2025

Published online: 21 March 2025

References

- Siegel RL, Giaquinto AN, Jemal A. Cancer statistics, 2024. *CA Cancer J Clin*. 2024;74(1):12–49.
- Zhu J, Liu A, Sun X, Liu L, Zhu Y, Zhang T, et al. Multicenter, randomized, phase III trial of neoadjuvant chemoradiation with capecitabine and irinotecan guided by UGT1A1 status in patients with locally advanced rectal cancer. *J Clin Oncol*. 2020;38(36):4231–9.
- Couwenberg AM, Burbach JPM, van Grevenstein WMU, Smits AB, Consten ECJ, Schiphorst AHW, et al. Effect of neoadjuvant therapy and rectal surgery on health-related quality of life in patients with rectal cancer during the first 2 years after diagnosis. *Clin Colorectal Cancer*. 2018;17(3):e499–512.
- Jones HJS, Cunningham C. Adjuvant radiotherapy after local excision of rectal cancer. *Acta Oncol*. 2019;58(sup1):S60–4.
- Vendrey V, Rivin Del Campo E, Modesto A, Jolnerowski M, Meillan N, Chiavassa S, et al. Rectal cancer radiotherapy. *Cancer Radiother*. 2022;26(1–2):272–8.
- Ma B, Gao P, Wang H, Xu Q, Song Y, Huang X, et al. What has preoperative radio(chemo)therapy brought to localized rectal cancer patients in terms of perioperative and long-term outcomes over the past decades? A systematic review and meta-analysis based on 41,121 patients. *Int J Cancer*. 2017;141(5):1052–65.
- Pelloski CE, Mahajan A, Maor M, Chang EL, Woo S, Gilbert M, et al. YKL-40 expression is associated with poorer response to radiation and shorter overall survival in glioblastoma. *Clin Cancer Res*. 2005;11(9):3326–34.
- Shao R, Francescone R, Ngernyuan N, Bentley B, Taylor SL, Moral L, et al. Anti-YKL-40 antibody and ionizing irradiation synergistically inhibit tumor vascularization and malignancy in glioblastoma. *Carcinogenesis*. 2014;35(2):373–82.
- Lei G, Zhang Y, Koppula P, Liu X, Zhang J, Lin SH, et al. The role of ferroptosis in ionizing radiation-induced cell death and tumor suppression. *Cell Res*. 2020;30(2):146–62.
- Jiang K, Yin X, Zhang Q, Yin J, Tang Q, Xu M, et al. STC2 activates PRMT5 to induce radioresistance through DNA damage repair and ferroptosis pathways in esophageal squamous cell carcinoma. *Redox Biol*. 2023;60:102626.
- Cheng G, Kong D, Hou X, Liang B, He M, Liang N, et al. The tumor suppressor, p53, contributes to radiosensitivity of lung cancer cells by regulating autophagy and apoptosis. *Cancer Biother Radiopharm*. 2013;28(2):153–9.
- Macedo-Silva C, Miranda-Goncalves V, Tavares NT, Barros-Silva D, Lencart J, Lobo J, et al. Epigenetic regulation of TP53 is involved in prostate cancer radioresistance and DNA damage response signaling. *Signal Transduct Target Ther*. 2023;8(1):395.
- Kang R, Kroemer G, Tang D. The tumor suppressor protein p53 and the ferroptosis network. *Free Radic Biol Med*. 2019;133:162–8.
- Liu K, Jin M, Ye S, Yan S. CHI3L1 promotes proliferation and improves sensitivity to cetuximab in colon cancer cells by down-regulating p53. *J Clin Lab Anal*. 2020;34(1):e23026.
- Huang T, Chen C, Du J, Zheng Z, Ye S, Fang S, et al. A tRF-5a fragment that regulates radiation resistance of colorectal cancer cells by targeting MKNK1. *J Cell Mol Med*. 2023;27(24):4021–33.
- Liu KT, Wan JF, Zhu J, Li GC, Sun WJ, Shen LJ, et al. Role of pelvic radiotherapy for locally advanced rectal cancer and synchronous unresectable distant metastases. *Cancer Radiother*. 2016;20(8):805–10.
- Boublikova L, Novakova A, Simsa J, Lohynska R. Total neoadjuvant therapy in rectal cancer: the evidence and expectations. *Crit Rev Oncol Hematol*. 2023;192:104196.
- Santivasi WL, Xia F. Ionizing radiation-induced DNA damage, response, and repair. *Antioxid Redox Signal*. 2014;21(2):251–9.
- Huang RX, Zhou PK. DNA damage response signaling pathways and targets for radiotherapy sensitization in cancer. *Signal Transduct Target Ther*. 2020;5(1):60.
- Lu C, El-Deiry WS. Targeting p53 for enhanced radio- and chemo-sensitivity. *Apoptosis*. 2009;14(4):597–606.
- Bohnke A, Westphal F, Schmidt A, El-Awady RA, Dahm-Daphi J. Role of p53 mutations, protein function and DNA damage for the radiosensitivity of human tumour cells. *Int J Radiat Biol*. 2004;80(1):53–63.
- Langland GT, Yannone SM, Langland RA, Nakao A, Guan Y, Long SB, et al. Radiosensitivity profiles from a panel of ovarian cancer cell lines exhibiting genetic alterations in p53 and disparate DNA-dependent protein kinase activities. *Oncol Rep*. 2010;23(4):1021–6.
- Brooks CL, Gu W. Ubiquitination, phosphorylation and acetylation: the molecular basis for p53 regulation. *Curr Opin Cell Biol*. 2003;15(2):164–71.
- Chan WM, Mak MC, Fung TK, Lau A, Siu WY, Poon RY. Ubiquitination of p53 at multiple sites in the DNA-binding domain. *Mol Cancer Res*. 2006;4(1):15–25.
- Xie Q, Li Z, Chen J. WDR5 positively regulates p53 stability by inhibiting p53 ubiquitination. *Biochem Biophys Res Commun*. 2017;487(2):333–8.
- Feng S, Huang Q, Deng J, Jia W, Gong J, Xie D, et al. DAB2IP suppresses tumor malignancy by inhibiting GRP75-driven p53 ubiquitination in colon cancer. *Cancer Lett*. 2022;532:215588.
- Dixon SJ, Lemberg KM, Lamprecht MR, Skouta R, Zaitsev EM, Gleason CE, et al. Ferroptosis: an iron-dependent form of nonapoptotic cell death. *Cell*. 2012;149(5):1060–72.
- Stockwell BR, Friedmann Angeli JP, Bayir H, Bush AI, Conrad M, Dixon SJ, et al. Ferroptosis: a regulated cell death nexus linking metabolism, redox biology, and disease. *Cell*. 2017;171(2):273–85.
- Saint-Germain E, Mignacca L, Vernier M, Bobbala D, Ilangumaran S, Ferbeyre G. SOCS1 regulates senescence and ferroptosis by modulating the expression of p53 target genes. *Aging*. 2017;9(10):2137–62.

30. Xu R, Wang W, Zhang W. Ferroptosis and the bidirectional regulatory factor p53. *Cell Death Discov.* 2023;9(1):197.
31. Jiang L, Kon N, Li T, Wang SJ, Su T, Hibshoosh H, et al. Ferroptosis as a p53-mediated activity during tumour suppression. *Nature.* 2015;520(7545):57–62.
32. Wang CK, Chen TJ, Tan GYT, Chang FP, Sridharan S, Yu CA, et al. MEX3A mediates p53 degradation to suppress ferroptosis and facilitate ovarian cancer tumorigenesis. *Cancer Res.* 2023;83(2):251–63.
33. Xie Y, Hou W, Song X, Yu Y, Huang J, Sun X, et al. Ferroptosis: process and function. *Cell Death Differ.* 2016;23(3):369–79.
34. Zeng C, Lin J, Zhang K, Ou H, Shen K, Liu Q, et al. SHARPIN promotes cell proliferation of cholangiocarcinoma and inhibits ferroptosis via p53/SLC7A11/GPX4 signaling. *Cancer Sci.* 2022;113(11):3766–75.
35. Zhang Y, Shi J, Liu X, Feng L, Gong Z, Koppula P, et al. BAP1 links metabolic regulation of ferroptosis to tumour suppression. *Nat Cell Biol.* 2018;20(10):1181–92.

Publisher's Note

Springer Nature remains neutral with regard to jurisdictional claims in published maps and institutional affiliations.